PHILOSOPHICAL TRANSACTIONS OF THE ROYAL SOCIETY B BIOLOGICAL SCIENCES

Air-Sea CO<latex>$_{2}$</latex> Transfer and the Carbon Budget of the North Atlantic [and Discussion]

J. L. Sarmiento, R. Murnane, C. Le Quere, R. Keeling and R. G. Williams

Phil. Trans. R. Soc. Lond. B 1995 **348**, 211-219
doi: 10.1098/rstb.1995.0063

Air–sea CO_2 transfer and the carbon budget of the North Atlantic

J. L. SARMIENTO, R. MURNANE AND C. LE QUÉRÉ

Atmospheric and Oceanic Sciences Program, Department of Geological and Geophysical Sciences, Princeton University, New Jersey 08544, U.S.A.

SUMMARY

A model simulation of the global carbon cycle demonstrates that the biological and solubility pumps are of comparable importance in determining the spatial distribution of annual mean air–sea fluxes in the Atlantic. The model also confirms that the impact of the (steady state) biological pump on the magnitude and spatial distribution of anthropogenic CO_2 uptake is minimal. An Atlantic Ocean carbon budget developed from analysis of the model combined with observations suggests that the air–sea flux of carbon is inadequate to supply the postulated large dissolved inorganic carbon export from the Atlantic. Other sources of carbon are required, such as an input from the Pacific via the Bering Strait and Arctic, river inflow, or an import of dissolved organic carbon.

1. INTRODUCTION

Volk & Hoffert (1985) introduced the terms solubility pump, carbonate pump, and soft-tissue pump, to denote the oceanographic processes that create and maintain concentration gradients in the ocean. We use the term 'biological pump' to denote the combination of the carbonate and soft-tissue pump. The emphasis of Volk & Hoffert's discussion was on the vertical concentration gradient of carbon. This paper presents Atlantic Ocean results from a new global carbon modelling study of the solubility and biological pumps. Discussion will cover vertical gradient processes, but the emphasis is on the horizontal. The first aim of this study was to understand how ocean circulation interacts with the heat and freshwater cycle (i.e. the solubility pump) and the biological pump to create features such as the large loss of CO_2 from the tropics and gain of CO_2 in high latitudes. Such an understanding is essential to the development of powerful new techniques for using the spatial distribution of carbon sources and sinks to constrain the total anthropogenic carbon budget (see Keeling *et al.* 1989*b*; Tans *et al.* 1990; Enting *et al.* 1993). A second major aim was to quantify the role of the biological pump in uptake of anthropogenic carbon from the atmosphere. The third major aim was to combine the model with observations to develop a carbon budget for the Atlantic Ocean. The paper begins with a discussion of the solubility and biological pumps followed by a discussion of their impact on oceanic anthropogenic carbon uptake, and concludes with a section that combines model results with observations to discuss the Atlantic Ocean carbon budget.

The role of the solubility and biological pumps is simulated in two parallel model runs, one of which includes solubility pump processes only, and a second 'combined' model that adds biological processes to the solubility pump model. The contribution of the biological pump is the difference between these two simulations. All simulations use the global ocean circulation model of Toggweiler *et al.* (1989*a*) as modified by Toggweiler and Samuels (1993). The model has an average horizontal resolution of about 4°, and 12 vertical levels of variable thickness. It is forced with annual mean climatic winds from Hellerman & Rosenstein (1983). Surface temperature and salinity are damped towards their observed annual mean climatic values obtained from Levitus (1982).

2. SOLUBILITY AND BIOLOGICAL PUMPS

Modelling the solubility pump requires: (i) an ocean circulation model with thermohaline forcing; (ii) solution of the carbon chemistry equations including temperature and salinity effects; and (iii) a model of gas exchange at the air–sea interface. For carbon chemistry we use the solution procedure of Peng *et al.* (1987), which requires specification of the total carbon content, alkalinity, temperature and salinity. We use the equilibrium constants of Goyet & Poisson (1989). Total carbon is modelled by fixing atmospheric CO_2 at its pre-industrial value of 278.2 ppm and allowing it to invade the ocean. For gas exchange we use the wind speed dependent formulation of Wanninkhof (1992) which is appropriate for (steady) winds and includes chemical enhancement. Wind speeds are taken from Esbensen & Kushnir (1981), and we take temperature and salinity from the ocean circulation model. Alkalinity follows salinity, with the global mean ratio of total alkalinity to salinity fixed at the observed value from GEOSECS data. No biological processes are included. The solubility pump simulation gives a global ocean carbon inventory of 37 409 Pg C (1 Pg = 1 Gt = 10^{15} g), as compared with the pre-industrial atmospheric inventory of 600 Pg C. The vast majority of the ocean inventory is in the form of bicarbonate and

Phil. Trans. R. Soc. Lond. B (1995) **348**, 211–219
Printed in Great Britain

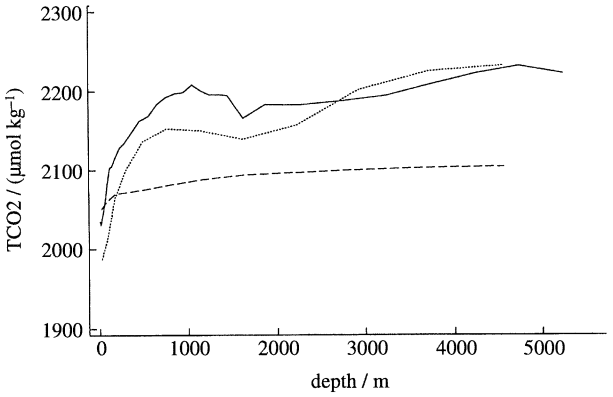

Figure 1. Atlantic Ocean mean vertical carbon profile predicted by the pre-industrial solubility and combined (biology plus solubility) models compared with observations from GEOSECS (shown as solid line). The dotted line denotes the combined model; the dashed line denotes the solubility pump. Note that the GEOSECS observations are contaminated with anthropogenic carbon concentrations which range from approximately 40 μmol kg^{-1} at the surface to near 0 at depth below the main thermocline.

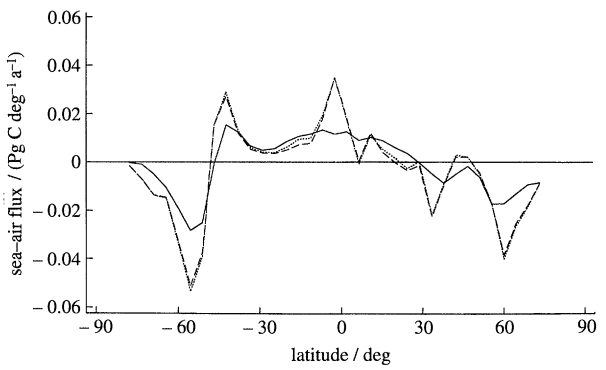

Figure 2. Zonally integrated Atlantic Ocean sea to air flux of carbon predicted by the solubility pump model (solid line). Positive values indicate an escape from the ocean to the atmosphere. The potential flux (shown by the dashed line) is the amount of carbon that would have to be taken up or released from surface water in order to equilibrate it with the atmosphere after changing its temperature (compare with Keeling *et al.* 1993). The potential flux from temperature and salinity changes is shown by the dotted line. Note that thermal forcing is the dominant term. The overall pattern results from warming in low latitudes and cooling in high latitudes. This pattern is broken between 30° and 60° by CO_2 escape to the atmosphere in both hemispheres due probably to spurious near shore upwelling driven by model lateral mixing across the western boundary currents (compare with Toggweiler *et al.* 1989*b*). The cold water upwelling to the surface is warmed and thus releases CO_2 to the atmosphere in a region where cooling is expected to predominate.

carbonate ions; if CO_2 did not react with water to form these ions, the ocean would have a capacity of less than 250 Pg C.

Figure 1 shows a vertical profile of Atlantic Ocean total carbon predicted by the model. The deep ocean concentration is of order 50 μmol kg^{-1} higher than the surface because of the higher solubility of CO_2 in the cold waters that fill the abyss. Also driven primarily by heat is the zonally integrated air–sea flux illustrated in figure 2. The loss of CO_2 from low latitudes and gain in high latitudes is as expected from the reduction of CO_2 solubility in regions of heating and the increase in solubility in regions of cooling. The effect of water fluxes on tracer concentrations also has an impact, though this is relatively small. Figure 2 shows a direct estimate of the 'potential' carbon flux, which we define as the flux that would occur if the ocean equilibrated instantaneously with atmospheric CO_2 content after experiencing a flux of heat or water (compare with Keeling *et al.* 1993; Watson *et al.* this volume). We use the model predicted heat and water fluxes for this calculation. The potential flux out of the ocean at the Equator is more than twice the actual flux. Because of the length of time it takes for oceanic CO_2 to equilibrate with the atmosphere (of order 0.7 year for a 50 m mixed layer), much of the potential flux does not actually occur until the Ekman transport has moved surface waters well away from the Equator. The poleward displacement of the equatorial potential flux leads to a reduction in the actual North Atlantic uptake over that predicted by the potential flux. For this reason, and because much of the water that experiences a potential flux is subducted before the flux actually occurs, we believe that the North Atlantic uptake of 0.75 Pg C a^{-1} estimated by Watson *et al.* (this volume) from the heat transport across 24° N is most likely an upper limit.

Figure 3 illustrates the impact of the solubility pump on the zonally integrated carbon transport by advection, mixing, and the 'virtual flux' (see caption for a definition). The surface outcropping of carbon transport streamlines in the Equatorial region is due to loss of CO_2 to the atmosphere. The carbon lost in this region is supplied primarily by shallow transport (< 200 m) from the subtropical and subpolar gyres of the northern hemisphere, where the outcropping streamlines indicate CO_2 uptake from the atmosphere. The deep export of carbon from the North Atlantic is less than 0.1 Pg C a^{-1}. The Atlantic sector of the Southern Ocean has a deep carbon transport exceeding 0.3 Pg C a^{-1}, but most of this is due to local overturning.

The combined model including the biological and solubility pumps is solved identically to the solubility pump, but with the addition of organic matter and $CaCO_3$ surface production, export, and deep remineralization. We do not include river input or sediment burial, as the constraints on the spatial distribution of these is poor and their impact on ocean concentrations is mainly local. Without such external sources and sinks the model will achieve a steady state ocean carbon cycle only when the globally integrated air–sea flux is 0.

Surface biological production of organic matter is modelled as in Sarmiento *et al.* (1988) and Najjar *et al.* (1992) by requiring that surface model predicted phosphate be relaxed towards the observed phosphate distribution. Organic carbon is produced with a Redfield mole ratio of 106:1 carbon to phosphorus. The global biological production of 11.9 Pg C a^{-1} goes half into particles and half into labile dissolved organic matter. Particles sink immediately below where they

PHILOSOPHICAL TRANSACTIONS OF THE ROYAL SOCIETY B BIOLOGICAL SCIENCES

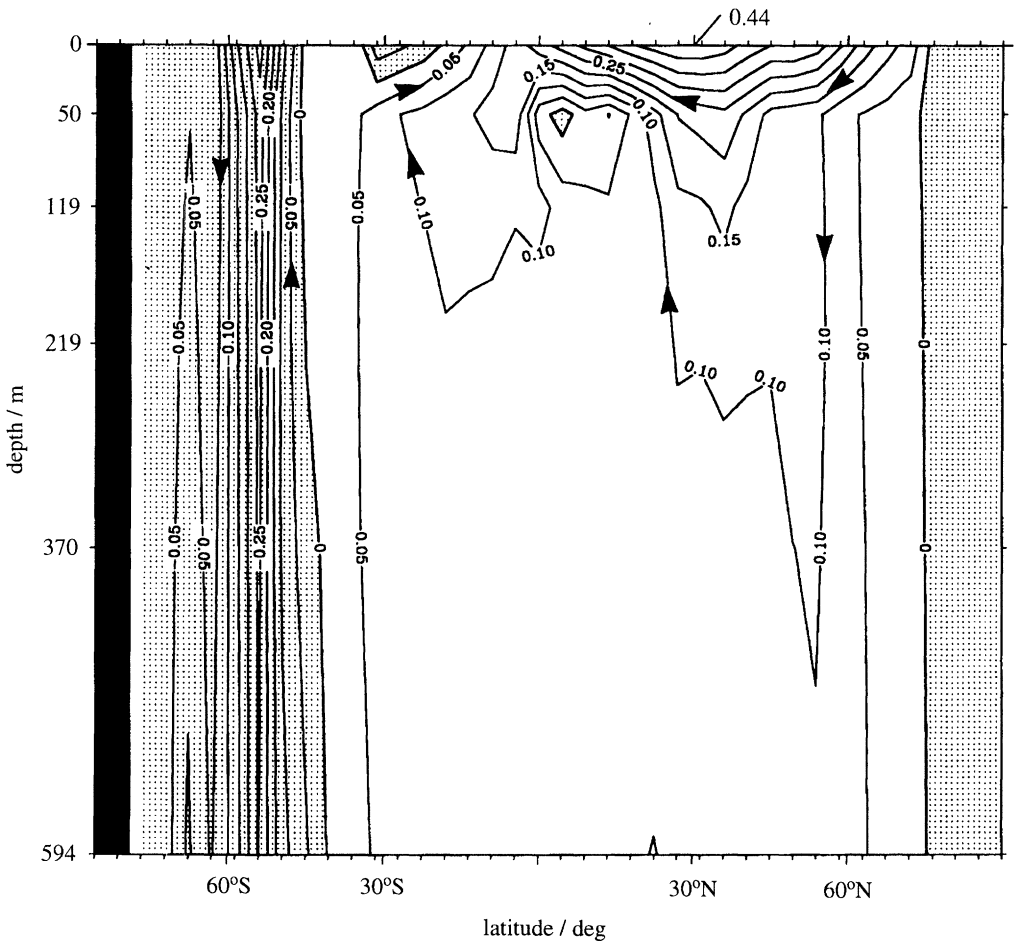

Figure 3. Impact of the solubility pump on zonally integrated carbon transport by diffusion, advection, and the 'virtual flux'. The contour interval is 0.05 Pg C a^{-1}. The arrows indicate the direction of the carbon transport. The mean total carbon concentration is subtracted off before doing the transport calculation in order to illustrate the impact of the solubility pump over what one would obtain if the carbon concentration were constant everywhere. The virtual flux is the addition or removal of surface salinity that is required to force the model prediction towards the observations (compare with Huang (1993) for a discussion of the complex problems this gives rise to). Tracer concentrations are corrected by the same fractional amount. The virtual flux represents the effect of freshwater fluxes across the air–sea interface. These are not modelled explicitly in our ocean general circulation model. One can think of the virtual flux as the transport that would exist within the ocean if the freshwater atmosphere–ocean fluxes and the corresponding oceanic transports were modelled explicitly.

are produced, and are remineralized instantaneously using the sediment trap scaling of Martin *et al.* (1987). Dissolved organic carbon is transported by the ocean circulation and mixing process. Remineralization of dissolved organic carbon is modelled as a first order decay with a mean life of 12.9 years. 2.2 Pg C of the dissolved organic matter is remineralized in the surface, giving an export production of 9.7 Pg C. Note that the global surface production of 11.9 Pg C a^{-1} is not equivalent to the primary production. The surface recycling of dissolved organic carbon that we include in this number is only a small fraction of the total recycling that would actually occur if we had a more complete biological model such as that of Fasham *et al.* (1990) and Sarmiento *et al.* (1993).

The global production and dissolution of $CaCO_3$ is modelled by requiring that the model horizontal mean alkalinity at each model level equal the observed horizontal mean obtained from GEOSECS observations. Both model and observations are first normalized to a constant salinity. The global $CaCO_3$ production and dissolution determined for each level is apportioned locally according to the magnitude of particulate organic carbon production and remineralization at that level. The flux of carbon predicted to leave the surface as $CaCO_3$ is 1.8 Pg C a^{-1}, giving an organic carbon to $CaCO_3$ carbon export ratio of 5.4.

The combined simulation gives a carbon inventory that is 2317 Pg (6.2%) greater than the solubility pump. As figure 1 shows, the cause of this is a large increase in deep ocean concentrations. Surface concentrations are actually lower because of the reduced alkalinity that results from $CaCO_3$ cycling, and lower alkalinity waters have less carbon holding capacity for a given pCO_2. The increased deep ocean concentrations in the presence of the biological pump are generally portrayed as resulting from the input of carbon from remineralization of organic matter at depth. An alternative view is that the deep ocean

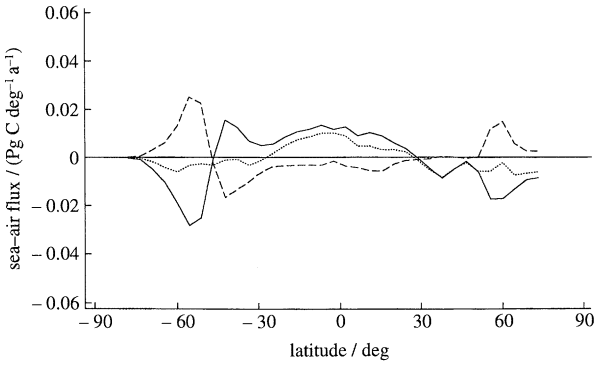

Figure 4. Zonally integrated Atlantic Ocean sea to air carbon fluxes for the solubility pump and combined simulations. The biological pump contribution (dashed line) is calculated by subtracting the solubility pump (shown as solid line) from the combined simulation (dotted line).

concentration increase is due to the requirement that the ocean carbon cycle be balanced. In the presence of a flux of organic matter from the surface to the abyss, and in the absence of an external source of carbon, the only way that a steady state can be achieved is by an upward transport of dissolved inorganic carbon in the ocean. The vertical gradient must increase to drive this upward flux, which requires an increase in deep ocean concentrations. This increase in deep ocean concentration is the biological pump's contribution to the air–sea balance of CO_2. A change in the efficiency of the biological pump would cause a large change in atmospheric CO_2 content by modifying the deep carbon content (see for example, Knox & McElroy 1984; Sarmiento & Toggweiler 1984; Siegenthaler & Wenk 1984; Sarmiento & Orr 1991; Kurz & Maier-Reimer 1993; Archer & Maier-Reimer 1994).

Figure 4 shows the air–sea CO_2 flux predicted by the combined simulation. We analyze the biological contribution by taking the difference between the combined simulation and the solubility pump simulation. In upwelling and deep convecting regions such as the Equatorial bands and subpolar gyres the carbon-enriched deep waters of the combined simulation outcrop at the surface. There the excess carbon will either escape to the atmosphere or be stripped out by biological uptake. The carbon that escapes to the atmosphere in such regions must be balanced by uptake in other regions of the ocean such as the subtropical gyres because in a steady state the globally integrated net air–sea flux must be zero. Figure 4 shows the expected biologically induced flux of CO_2 to the atmosphere in the high latitudes of the Atlantic Ocean, balanced by uptake elsewhere. The Equatorial upwelling band does not show a flux to the atmosphere because here the organisms strip out the nutrients relatively efficiently. The Pacific, by contrast, does have a biologically induced Equatorial flux to the atmosphere. The magnitude of the biologically induced air–sea fluxes is very large; in the high latitudes it is almost of the same magnitude as the solubility pump. The two fluxes are opposite in sign and thus almost cancel eachother, giving a greatly reduced flux over what one would expect with the solubility pump alone.

3. ROLE OF PUMPS IN OCEANIC UPTAKE OF ANTHROPOGENIC CARBON

The oceanic uptake of anthropogenic carbon is simulated by fixing the atmospheric CO_2 content at its observed concentration and allowing it to invade the ocean. The CO_2 concentration history is determined from trapped air bubbles in the South Pole (Siegenthaler *et al.* 1988) and Siple ice cores (Neftel *et al.* 1982; Friedli *et al.* 1986), and measurements made at Mauna Loa (Keeling & Whorf 1991). Figure 5 shows the spatial distribution of the anthropogenic carbon fluxes obtained with the combined model in the year 1990; the flux is into the ocean everywhere. When summed to the pre-industrial fluxes of figure 4, we see that the anthropogenic flux increases the pre-industrial uptake in the high latitudes but reduces the pre-industrial efflux at the Equator. Figure 5 also shows the spatial distribution of the CO_2 uptake obtained with the solubility pump model alone, and the contribution of the biological pump obtained from the difference between the solubility pump model and the combined model. From this we see that the contribution of the biological pump to the spatial distribution of the anthropogenic uptake is very small everywhere except in high latitudes, where the magnitude is about 20 % of the solubility pump. The small contribution of the biological pump is consistent with earlier work showing that the rate limiting step of anthropogenic CO_2 uptake is ocean circulation and mixing (Sarmiento *et al.* 1992). The contribution of the biological pump to the integrated uptake of anthropogenic carbon is also very small. Indeed, the cumulative global uptake is less in the combined model than in the solubility pump model (by 4.9 %) because of the diminished carbon holding capacity of surface waters that results from reduced surface alkalinity.

The biological pump has a very small direct impact on oceanic uptake of anthropogenic carbon. The role that it plays is in determining the spatial distribution of present air–sea CO_2 fluxes, and in creating a potential for large changes in the air–sea carbon balance through modifications of the biological pump.

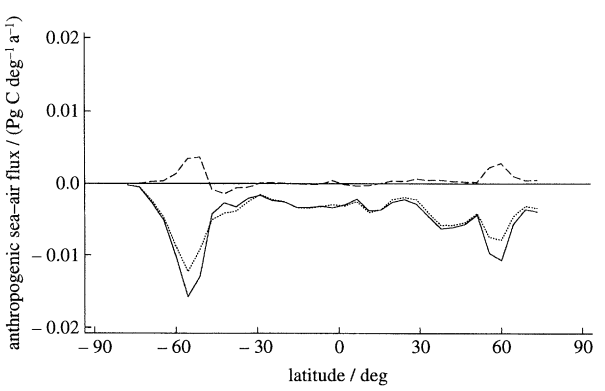

Figure 5. Zonally integrated Atlantic Ocean anthropogenic carbon uptake in 1990. Solid line denotes the solubility pump; dashed line denotes biological pump; dotted line denotes the combined model.

PHILOSOPHICAL TRANSACTIONS OF THE ROYAL SOCIETY B BIOLOGICAL SCIENCES

4. ATLANTIC CARBON BUDGET

A complete carbon budget for the Atlantic must consider input of carbon by rivers, burial in sediments and gas exchange at the air–sea interface as well as transport of dissolved inorganic carbon (DIC) and dissolved organic carbon (DOC) across both the northern and southern boundaries of the basin. An assumption implicit in most studies is that the two major terms of the budget are DIC export to the south balanced by CO_2 uptake from the atmosphere. We show here that a more likely scenario is that the southwards DIC export is balanced by DIC import from the Pacific via the Arctic with a possible contribution from rivers and DOC. We consider each term in turn beginning with the southwards DIC transport.

A number of studies have used hydrographic and total carbon measurements to estimate carbon transport across various sections in the Atlantic. Brewer *et al.* (1989) obtained an outflow of 0.26 Pg C a^{-1} using observations at 25° N. Watson *et al.* (this volume) note that Brewer subsequently proposed an anthropogenic carbon correction that gives a pre-industrial southwards transport of 0.41 Pg C a^{-1}. Robbins (1994) has estimated a southwards transport of 0.3 Pg C a^{-1} at 24° S in the Atlantic. His pre-industrial estimate is approximately 0.5 Pg C a^{-1}. Schlitzer (1989) gives the net southwards export from the Atlantic and Arctic as 0.1 to 1.1 Pg C a^{-1} across 10° S. He reports this as an uptake from the atmosphere, but strictly speaking it is calculated as the divergence of the oceanic transport of dissolved inorganic carbon. If we leave out the highest transports of Schlitzer (1989), these estimates taken together give a southwards Atlantic Ocean DIC export of roughly 0.4 ± 0.3 Pg C a^{-1} today, and 0.6 ± 0.3 Pg C a^{-1} before the industrial revolution. This range includes the pre-industrial outflow of 0.6 Pg C a^{-1} estimated by Broecker and Peng (1992) using an analysis of the properties of deep waters involved in the thermohaline overturning. Figure 6 shows all these Atlantic DIC transport estimates together with additional estimates by Martel & Wunsch (1993) and the results of our model simulations. The model agrees reasonably well with the transport estimates in the mid-latitudes of the northern hemisphere, but it is too low in the far north and gives an export of less than 0.1 Pg C a^{-1} out of the Atlantic in the south. The model predicted export is at the very edge of the range of estimates reported by Schlitzer (1989), though it is well within the uncertainty range reported by Martel & Wunsch (1993).

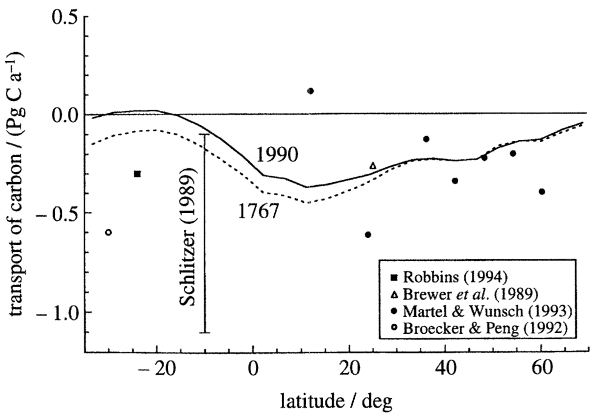

Figure 6. Northward transport of carbon in the Atlantic Ocean. The symbols are advective transport estimates obtained by analysis of zonal sections by Brewer *et al.* (1989), Schlitzer (1989), Martel & Wunsch (1993) and Robbins (1994). Broecker & Peng (1992) and Watson *et al.* (1995) use a different approach for their calculations. All the transport estimates are for the present ocean except Broecker & Peng, which is for the pre-industrial ocean. The lines are model transports, including advection, diffusion and the virtual transport flux. See figure 3 for a discussion of the virtual flux. Model diffusion represents processes on spatial scales smaller than 4°, most of which we presume would be captured by high resolution section measurements used for transport estimates. Model transport is shown for the pre-industrial steady state (labelled 1767), and for 1990. The difference between these two lines is the anthropogenic contribution.

Table 1. *Integrated air–sea fluxes (Pg C a^{-1}) from Takahashi compared to model.*

(The column labelled C-14 uses a gas exchange coefficient based on calibration with oceanic observations of bomb radiocarbon (Tans *et al.* 1990); the column labelled L & M uses Liss & Merlivat (1986). Our study uses the bomb radiocarbon calibrated gas exchange coefficient of Wanninkhof (1992). A positive sign signifies loss from the ocean to the atmosphere.)

	Takahashi *et al.* (this volume)		
latitude	C-14	L & M	this study
42° N to 78° N	−0.48	−0.23	−0.34
18° N to 42° N	−0.22	−0.10	−0.14
18° S to 18° N	+0.17	+0.08	+0.14
total	−0.53	−0.25	−0.34

Could a large Atlantic DIC export, if it exists, be supplied by atmospheric CO_2 uptake? Takahashi *et al.* (this volume) use air–sea CO_2 difference measurements and a simple model interpolation scheme to obtain an 18° S to 78° N atmospheric CO_2 uptake of 0.25 to 0.53 Pg C a^{-1} for 1990, with the range representing two estimates of the wind-speed dependent gas exchange coefficient (see table 1). However, a large portion of the 1990 uptake is due to the anthropogenic transient. We estimate from our models that the anthropogenic uptake between 18° S and 78° N is 0.38 Pg C a^{-1}. The implication is that the pre-industrial air–sea uptake flux must have been extremely small, or that there may even have been an escape of CO_2 to the atmosphere. This is most likely the case even if the thermal skin correction proposed by Robertson & Watson (1992) is included. Watson *et al.* (this volume), who carefully analyze some of the potential problems with the Takahashi *et al.* (this volume) technique, have used an alternative approach to estimate an uptake of 0.7 Pg C a^{-1} for the region north of 15° N for the mid 1980s. Their uptake is at the upper limit of the uptake of 0.33–0.70 Pg C a^{-1} proposed by Takahashi *et al.* (this volume) for the region between 18° N and 78° N (see table 1). We conclude that the air–sea flux for the

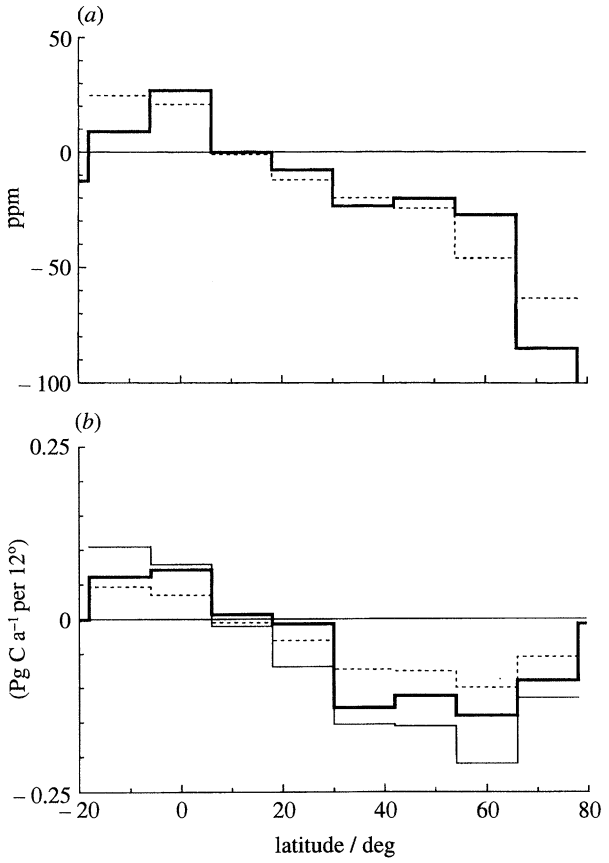

Figure 7. (*a*) Atlantic Ocean mean sea–air pCO_2 difference from observations of Takahashi *et al.* (this volume) (dashed line) and from the model simulation (solid line). (*b*) Zonally integrated Atlantic Ocean sea to air flux in 1990. The bold line shows the model estimation; the dashed line and fine line are from Takahashi *et al.* (this volume). The fine line uses a gas exchange coefficient based on calibration with oceanic observations of bomb radiocarbon (Tans *et al.* 1990), and the dashed line uses Liss & Merlivat (1986). Both use the same observations of sea–air pCO_2 difference.

Table 2. *Annual mean sea–air pCO_2 difference in ppm*

latitude	Takahashi *et al.* (this volume)	model result
42° N to 78° N	−40.3	−42.6
18° N to 42° N	−15.8	−14.0
18° S to 18° N	+14.8	+13.7

Atlantic including the region between 18° S and 18° N is of order 0.4 ± 0.2 Pg C a^{-1} today, and that it was of order 0.0 ± 0.2 Pg C a^{-1} before the industrial revolution. The pre-industrial air–sea flux is thus insufficient to supply the postulated large southwards transport of inorganic carbon of 0.6 ± 0.3 Pg C a^{-1}.

Our model simulation of atmosphere–ocean exchange processes is remarkably consistent with that of Takahashi *et al.* (this volume). Figure 7*a* and table 2 show that the sea–air pCO_2 difference predicted by the model is almost identical to the annual mean obtained by Takahashi *et al.* from his analysis of measurements. The only area of disagreement is in the far north and south where Takahashi *et al.* do not have as many measurements. Figure 7*b* and table 1 show that the

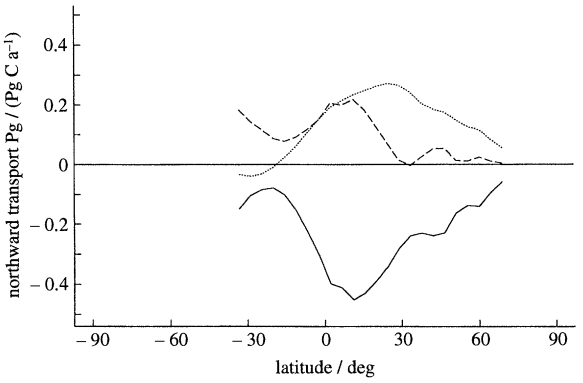

Figure 8. Northward transport of DIC (solid line) and DOC (dashed line)in the pre-industrial model Atlantic Ocean. The ocean transport is the sum of advection, diffusion and the virtual flux. The atmospheric transport (dotted line) component shown in the figure is only that portion of the total atmospheric transport that is attributable to the Atlantic Ocean carbon cycle.

air–sea flux of −0.34 Pg C a^{-1} predicted by our model falls between Takahashi's flux estimates of −0.25 and −0.53 Pg C a^{-1} based on two gas exchange models. The gas exchange model we use (Wanninkhof 1992) is radiocarbon based, as is the Tans *et al.* (1990) model used by Takahashi *et al.* to obtain his higher flux of −0.53 Pg C a^{-1}. One reason our estimate is lower is because the Wanninkhof (1992) gas exchange coefficient is below that of Tans *et al.* (1990) for wind speeds between about 4.5–13 ms^{-1}. However, this will only explain part of the difference. Other possible explanations remain to be explored such as the role of seasonality, which is included in Takahashi's estimate but not in ours. The total North Atlantic uptake in our model from 18° S to 78° N is 0.34 Pg C a^{-1} in 1990. However, the anthropogenic CO_2 uptake is 0.38 Pg C a^{-1}. The pre-industrial Atlantic thus releases 0.04 Pg C a^{-1} to the atmosphere.

We conclude that if there is a large export of dissolved inorganic carbon from the Atlantic it must be supplied by another mechanism such as an inflow of dissolved organic carbon or riverine carbon, or an input from the Pacific through the Bering Straits. As a measure of the first of these mechanisms we show in figure 8 the DOC transport predicted by the model along with the DIC transport and the meridionally integrated air–sea flux. The integrated air–sea flux is equal to the atmospheric carbon transport that would be required to balance the ocean carbon cycle for the North Atlantic. We see from this plot that the atmospheric transport is actually towards the south at 30° S, contrary to the implication of the Keeling *et al.* (1989*a*) Mauna-Loa-South Pole analysis, and despite the fact that the ocean transport of DIC is also to the south. Both the atmospheric and ocean DIC transport are supplied by a northwards transport of DOC. Rintoul & Wunsch (1991) estimate a dissolved organic nitrogen to inorganic nitrogen conversion of 119 ± 35 kmol s^{-1} in the region between 24° N and 36° N. If we use a Redfield ratio of 117 organic carbon atoms to 16 nitrogen atoms, this would imply a net DOC import of 0.33 Pg C a^{-1}. These results suggest that it is critical to

PHILOSOPHICAL TRANSACTIONS OF THE ROYAL SOCIETY B BIOLOGICAL SCIENCES

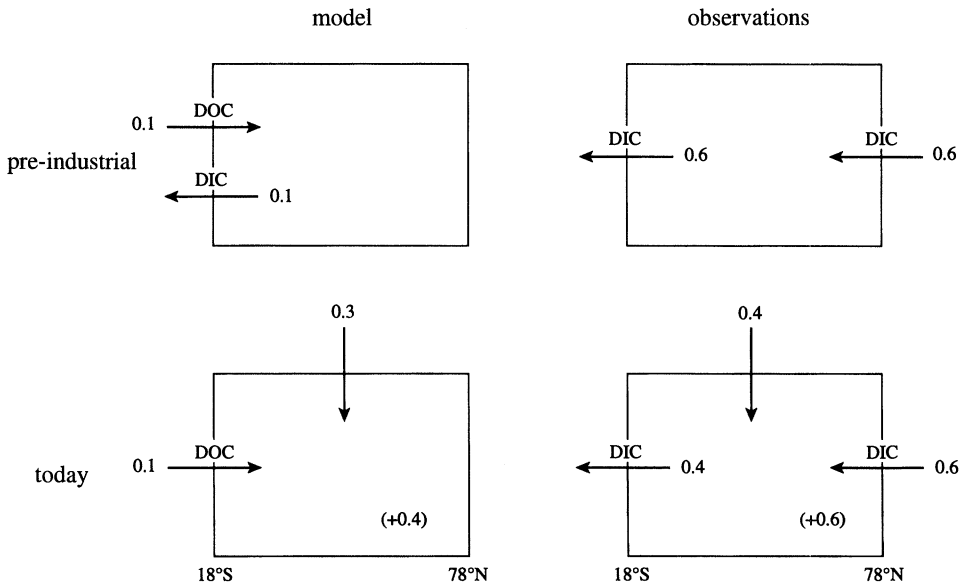

Figure 9. Schematic carbon budget for the Atlantic Ocean between 18° S and 78° N. The model budget is based entirely on results obtained by the model described in the text. The 'observed' carbon budget is based on observational estimates of carbon transport out of the South Atlantic, net carbon inflow to the North Atlantic estimated from the net flow of water through the Arctic from the Bering Sea, and Takahashi *et al.*'s (this volume) sea–air flux estimate for the present. The anthropogenic component of the present sea–air flux is estimated from our model results, and the accumulation rate in the present ocean is an estimate based on differencing the numbers.

include DOC measurements in the sections used to estimate carbon transports.

What about river input? Sarmiento & Sundquist (1992) summarized studies estimating that the total riverine carbon input to the world oceans is 0.4–0.7 Pg C a^{-1}. A substantial fraction of this must occur in the Atlantic, where most of the rivers of the world discharge. We are not aware of a breakdown of the riverine carbon budget that would allow us to estimate the Atlantic input directly. Watson *et al.* (this volume) suggest that 10% of the riverine flux plays a role in the Atlantic DIC budget, but there is nothing to substantiate this number. The total riverine carbon input is certainly large enough to supply the southwards flux suggested by the ocean transport calculations.

Finally we have the possibility of transport of DIC through the Arctic from the Bering Straits. L. Lundberg & P. Haugan (personal communication) have estimated a carbon through flow of 0.63 Pg C a^{-1} from the product of the net water flow into the Arctic of 0.8×10^6 m^3 s^{-1} (Coachman & Aagard 1988) times the DIC concentration of 2020–2040 μmol kg^{-1} (Anderson *et al.* 1990) and the density of 1.026 kg l^{-1} (Stigebrandt 1984). This is a very large number indeed, and would have quite a substantial impact on the Atlantic carbon budget. Our model has essentially no flow through the Bering Strait. Additional inputs of carbon to the Arctic, estimated to be of order 0.2 Pg C a^{-1} by Anderson *et al.* (1990), would also have to be considered. Adding these numbers to the transports shown in figure 6 would give a very large southwards DIC transport such as those suggested by other studies.

Figure 9 summarizes the carbon budget for the Atlantic Ocean obtained by the model and by the analysis of observations that we have gone through above. We conclude that there may exist a large southwards transport of carbon out of the Atlantic Ocean. However, this transport does not appear to be supplied by atmospheric CO_2 uptake, but rather by some unknown combination of northwards DOC transport, riverine input, and almost certainly a substantial flux from the Arctic due to input from the Pacific via the Bering Strait.

We appreciate the assistance of Jason Olszewski in preparation of the manuscript. This research was supported by a jointly funded project of the Electrical Power Research Institute (Grant no. RP 8011 17) and New Jersey Marine Sciences Consortium (Sea Grant grant no. RM/2 from the Coastal Ocean Program of the NOAA to the New Jersey Marine Sciences Consortium), by the National Science Foundation Joint Global Ocean Flux Program (OCE-9314707), and by the U.S. Department of Energy under contract DE-FG02–90ER61052. The views expressed herein are those of the authors and do not necessarily reflect the views of any of the agencies that funded the work.

REFERENCES

Anderson, L.G., Dyrssen, D. & Jones, E.P. 1990 An assessment of the transport of atmospheric CO_2 into the Arctic Ocean. *J. geophys. Res.* **95**, 1703–1711.

Archer, D. & Maier-Reimer, E. 1994 Effect of deep–sea sedimentary calcite preservation on atmospheric CO_2 concentration. *Nature, Lond.* **367**, 260–263.

Brewer, P.G., Goyet, C. & Dyrssen, D. 1989 Carbon dioxide transport by ocean currents at 25-N latitude in the Atlantic Ocean. *Science, Wash.* **246**, 477–479.

Broecker, W.S. & Peng, T.-H. 1992 Interhemispheric transport of carbon dioxide by ocean circulation. *Nature, Lond.* **356**, 587–589.

Coachman, L.K. & Aagard, K. 1988 Transports through Bering Strait: annual and interannual variability. *J. geophys. Res.* **93**, 15535–15539.

PHILOSOPHICAL TRANSACTIONS OF THE ROYAL SOCIETY B BIOLOGICAL SCIENCES

Enting, I.G., Trudinger, C.M., Francey, R.J. & Granek, H. 1993 Synthesis inversion of atmospheric CO_2 using the GISS tracer transport model. *CSIRO, Aust. Div. Atmos. Res. Tech. Pap.* **29**, 1–44.

Esbensen, S.K. & Kushnir, Y. 1981 The heat budget of the global ocean: an atlas based on estimates from surface marine observations. *Clim. Res. Inst. Rep.* **29**. Corvallis: Oregon State University.

Fasham, M.J.R., Ducklow, H.W. & McKelvie, S.M. 1990 A nitrogen-based model of plankton dynamics in the oceanic mixed layer. *J. mar. Res.* **48**, 591–639.

Friedli, H., Lötscher, H., Oeschger, H., Siegenthaler, U. & Stauffer, B. 1986 Ice core record of the $^{13}C/^{12}C$ ratio of atmospheric carbon dioxide in the past two centuries. *Nature, Lond.* **324**, 237–238.

Goyet, C. & Poisson, A. 1989 New determination of carbonic acid dissociation constants in seawater as a function of temperature and salinity. *Deep Sea Res.* **36**, 1635–1654.

Hellerman, S. & Rosenstein, M. 1983 Normal monthly wind stress over the world ocean with error estimates. *J. phys. Oceanogr.* **13**, 1093–1104.

Huang, R.X. 1993 Real freshwater flux as a natural boundary condition for the salinity balance and thermohaline circulation forced by evaporation and precipitation. *J. phys. Oceanogr.* **23**, 2428–2446.

Keeling, C.D., Bacastow, R.B., Carter, A.F., Piper, S.C., Whorf, T.P., Heimann, M., Mook, W.G. & Roeloffzen, H. 1989*a* A three-dimensional model of atmospheric CO_2 transport based on observed winds: 1 Analysis of observational data. In *Aspects of climate variability in the Pacific and the western Americas AGU monograph*, vol. 55 (ed. D.H. Peterson), pp. 165–236. Washington D.C.: AGU.

Keeling, C.D., Piper, S.C. & Heimann, M. 1989*b* A three-dimensional model of atmospheric CO_2 transport based on observed winds: 4 Mean annual gradients and interannual variations. In *Aspects of climate variability in the Pacific and the western Americas AGU monograph*, vol. 55 (ed. D. H. Peterson), pp. 305–363. Washington D.C.: AGU.

Keeling, C.D. & Whorf, T.P. 1991 Mauna Loa. In *Trends '91: a compendium of data on global change*, vol. ORNL/CDIAC-46 (ed. T. A. Boden, R.J. Sepanski & F.W. Stoss), pp. 12–14. Carbon Dioxide Information Analysis Center, Oak Ridge National Laboratory, Tennessee.

Keeling, R.F., Najjar, R.G. Bender, M.L. & Tans, P.P. 1993 What atmospheric oxygen measurements can tell us about the global carbon cycle. *Global Biogeochem. Cycles* **7**, 37–68.

Knox, F. & McElroy, M. 1984 Changes in atmospheric CO_2, influence of marine biota at high latitudes. *J. geophys. Res.* **89**, 4629–4637.

Kurz, K.D. & Maier-Reimer, E. 1993 Iron fertilization of the austral ocean–the hamburg model assessment. *Global Biogeochem. Cycles* **7**, 229–244.

Levitus, S. 1982 Climatological atlas of the world ocean (professional paper), vol. 13. Rockville, Maryland: National Oceanic and Atmospheric Administration.

Liss, P.S. & Merlivat, L. 1986 Air–sea gas exchange rates: introduction and synthesis. In *The role of air–sea exchange in geochemical cycling* (ed. P. Buat-Menard), pp. 113–127. D. Reidel Publishing Co.

Martel, F. & Wunsch, C. 1993 The North Atlantic circulation in the early 1980s -an estimate from inversion of a finite-difference model. *J. phys. Oceanogr.* **23**, 898–924.

Martin, J.H., Knauer, G.H., Karl, D.M. & Broenkow, W.W. 1987 VERTEX: Carbon cycling in the northeast Pacific. *Deep Sea Res.* **34**, 267–285.

Najjar, R.G., Sarmiento, J.L. & Toggweiler, J.R. 1992 Downward transport and fate of organic matter in the oceans: simulations with a general circulation model. *Global Biogeochem. Cycles* **6**, 45–76.

Neftel, A., Oeschger, H., Schwander, J., Stauffer, B. & Zumbrunn, R. 1982 Ice core measurements give atmospheric pCO_2 content during the past 40,000 years. *Nature, Lond.* **295**, 220–223.

Peng, T.H., Takahashi, T. & Broecker, W.S. 1987 Seasonal variability of carbon dioxide, nutrients and oxygen in the northern North Atlantic surface water: observations and a model. *Tellus* **39**, 439–458.

Rintoul, S. & Wunsch, C. 1991 Mass, heat, oxygen, and nutrient fluxes and budgets in the North Atlantic Ocean. *Deep Sea Res.* **38**, 355–377. (Suppl.)

Robertson, J.E. & Watson, A.J. 1992 Thermal skin effect of the surface ocean and its implications for CO_2 uptake. *Nature, Lond.* **358**, 738–740.

Sarmiento, J.L. & Orr, J.C. 1991 Three-dimensional simulations of the impact of Southern Ocean nutrient depletion on atmospheric CO_2 and ocean chemistry. *Limnol. Oceanogr.* **36**, 1928–1950.

Sarmiento, J.L., Orr, J.C. & Siegenthaler, U. 1992 A perturbation simulation of CO_2 uptake in an ocean general circulation model. *J. geophys. Res.* **97**, 3621–3646.

Sarmiento, J.L., Slater, R.D., Fasham, M.J.R., Ducklow, H.W., Toggweiler, J.R. & Evans, G.T. 1993 A seasonal three-dimensional ecosystem model of nitrogen cycling in the North Atlantic euphotic zone. *Global Biogeochem. Cycles* **7**, 417–450.

Sarmiento, J.L. & Sundquist, E.T. 1992 Revised budget for the oceanic uptake of anthropogenic carbon dioxide. *Nature, Lond.* **356**, 589–593.

Sarmiento, J.L. & Toggweiler, J.R. 1984 A new model for the role of the oceans in determining atmospheric pCO_2. *Nature, Lond.* **308**, 621–624.

Sarmiento, J.L., Toggweiler, J.R. & Najjar, R. 1988 Ocean carbon cycle dynamics and atmospheric pCO_2. *Phil. Trans. R. Soc. Lond.* A **325**, 3–21.

Schlitzer, R. 1989 Modeling the nutrient and carbon cycles of the North Atlantic 2. New production, particle fluxes, CO_2 gas exchange, and the role of organic nutrients. *J. geophys. Res.* **94**, 12, 781–12, 794.

Siegenthaler, U., Friedli, H., Loetscher, H., Moor, E., Neftel, A., Oeschger, H. & Stauffer, B. 1988 Stable-isotope ratios and concentration of CO_2 in air from polar ice cores. *Ann. Glaciol.* **10**, 1–6.

Siegenthaler, U. & Wenk, T. 1984 Rapid atmospheric CO_2 variations and ocean circulation. *Nature, Lond.* **308**, 624–625.

Stigebrandt, A. 1984 The North Pacific: a global-scale estuary. *J. phys. Oceanogr.* **14**, 464–470.

Tans, P.P., Fung, I.Y. & Takahashi, T. 1990 Observational constraints on the global atmospheric CO_2 budget. *Science, Wash.* **247**, 1431–1438.

Toggweiler, J.R., Dixon, K. & Bryan, K. 1989*a* Simulation of radiocarbon in a coarse-resolution world ocean model. 1. Steady state prebomb distributions. *J. geophys. Res.* **94**, 8217–8242.

Toggweiler, J.R., Dixon, K. & Bryan, K. 1989*b* Simulation of radiocarbon in a coarse-resolution world ocean model. 2. Distributions of bomb–produced ^{14}C. *J. geophys. Res.* **94**, 8243–8264.

Toggweiler, J.R. & Samuels, B. 1993 Is the magnitude of the deep outflow from the Atlantic Ocean actually governed by southern hemisphere winds? In *The global carbon cycle* (ed. M. Heimann), pp. 333–366, Berlin: Springer-Verlag.

Volk, T. & Hoffert, M.I. 1985 Ocean carbon pumps: analysis of relative strengths and efficiencies in ocean-

PHILOSOPHICAL TRANSACTIONS OF THE ROYAL SOCIETY B BIOLOGICAL SCIENCES

driven atmospheric CO_2 changes. In *The carbon cycle and atmospheric CO_2: natural variations archean to present* (ed. E.T. Sundquist & W.S. Broecker), pp. 99–110.

Wanninkhof, R. 1992 Relationship between wind speed and gas exchange over the ocean, *J. geophys. Res.* **97**, 7373–7383.

Discussion

R. Keeling (*Scripps Institution of Oceanography, La Jolla, California, U.S.A.*). First, I wish to point out that my revisiting the Broecker & Peng (1992) approach led to a transport by the conveyor circulation of 0.4 Gt C a^{-1}, mainly because I assumed 13 Sv versus the 20 Sv assumed by Broecker & Peng. Secondly, the authors' maps of $\Delta\Sigma CO_2$ showed larger differences between high and low latitudes in the southern hemisphere than Broecker & Peng and this suggests a possible problem with the GCM model within the southern hemisphere itself.

J.L. Sarmiento In answer to the first part: the revised estimate of Broecker & Peng's (1992) results is still well within the uncertainty of the carbon transport estimates reported by Schlitzer (1989) and Martel & Wunsch (1993). I have no problem with it. Secondly, our maps of $\Delta\Sigma CO_2$ show about 75 μmol l^{-1} higher carbon in the Southern Ocean than at the Equator, whereas Broecker & Peng are only about 25 μmol l^{-1} higher. This probably is an indication of problems with our model. Figure 4 shows that the solubility pump in the Southern Ocean takes up CO_2. One possible problem is that the cooling in our model Southern Ocean is too great. The simulation in the Southern Indian Ocean does indeed show an excessively large transport of warm waters to the south that could be the cause of too much cooling. Another possibility is that the biologically induced flux from the ocean to the atmosphere in the Southern Ocean is too weak. The surface phosphate data that we use to force our model is the mean of all data available and must therefore have a summertime (i.e. low) bias in the high latitudes. If we force the phosphate to a value that is low, this will reduce the biologically induced outwards flux of CO_2 from the ocean to the atmosphere and thus result in too high carbon in the Southern Ocean.

R. G. Williams (*Oceanography Laboratories, University of Liverpool, U.K.*). I support the emphasis of the modelling study on the inclusion of horizontal advection, rather than the traditional focus on vertical advection and mixing in geochemical studies. I believe that incorporating seasonality in the global model should increase the solubility pump in the North Atlantic and Southern Ocean. The seasonal cycle controls the ventilation process, which shows a biased transfer of cold, winter waters from the mixed layer into the main thermocline. Although CO_2 has a long equilibration timescale, Follows *et al.* (1994) show that there is an integrated effect of the seasonal cycle leading to an enhanced ocean take up of CO_2. We find that the air–sea CO_2 flux over the North Atlantic subtropical gyre is increased by 0.2 Gt C a^{-1} in a seasonal integration of an inorganic carbon model, compared with an annual-mean integration. This seasonal enhancement might be masked in numerical models that are over diffusive, rather than advective.

Reference

Follows, Williams & Marshall 1994 Subduction of carbon in the subtropical gyre of the North Atlantic. *J. mar. Res.* (Submitted.)

J. L. Sarmiento. My reason for emphasizing the horizontal transport of carbon is because, aside from the use of tracers such as oxygen and carbon isotopes, I believe that the study of the spatial distribution of carbon sources and sinks is where we stand to learn the most about the global carbon budget at the present time. Our model study will clearly not be complete until we have determined the influence of seasonality on the carbon budget. I suspect the impact will not be large because of the fact that the heat, water, and biological nutrient budgets do not differ dramatically in model simulations that we have done where seasonality has been included.

PHILOSOPHICAL TRANSACTIONS OF THE ROYAL SOCIETY B BIOLOGICAL SCIENCES